4.2.14 Test Campaign 13 (9/14 to 9/28/99)

The Thirteenth Slipstream test was structured to support the objectives stated for Test No. 10 in the original test matrix plan (see Table I-1 in Appendix I).

For this test, seven (7) 1.5-meter long candles constructed of metal fiber media were evaluated in the slipstream unit. It was a follow-up to Test Campaigns 8 and 10 where a new media alloy and filter construction were being studied. The only change in these filters was a new recipe for laying down the media fibers. The alteration was made in an attempt to further enhance the blinding characteristics of the filter used in Test Campaign 10. The test was scheduled for 250 hours of syngas operation. It lasted 300 hours in duration.

The filters for this study were constructed with a new media alloy being evaluated for use in the commercial vessels. The primary objective of this study was to evaluate the blinding characteristics for the new media recipe. Figure 4.2.14.1 shows the filter differential pressure as a function of time over the test period. A linear fit of the data predicts a filter blinding life of 7,350 hours. This rate is within the acceptable level required for the WREL HGF. From a blinding standpoint, this filter demonstrates good performance and would be suitable for the WREL process. Also shown on Figure 4.2.14.1 are the three media recipes tested using this new alloy. The data clearly shows that the recipe (#2) used in Test Campaign 10 offers the best blinding life.

Over the course of the study there was no appreciable gain in backup filter resistance. Consequently, the filtration efficiency for these candles is deemed to be within the acceptable range for the WREL process.

The test concluded a series of studies (also see Test Campaigns 8 and 10) aimed at developing a new alloy filter that would ultimately serve as an upgrade to the "standard" candle filter used at the Wabash facility. When compared to the standard media, the new alloy provides nearly twice the corrosion life and has equally as good or better blinding characteristics. In the early stages of development, problems in fabrication were recognized and corrected. As result the filter has proven to be highly reliable in the commercial process. Along with this effort a new configuration was developed for fixing the filters within the vessel tubesheet. The changes also incorporate an improved system for holding fail-safe devices within the filters. The improvements have significantly increased filter life and greatly reduced the overall maintenance time required for the commercial HGF.

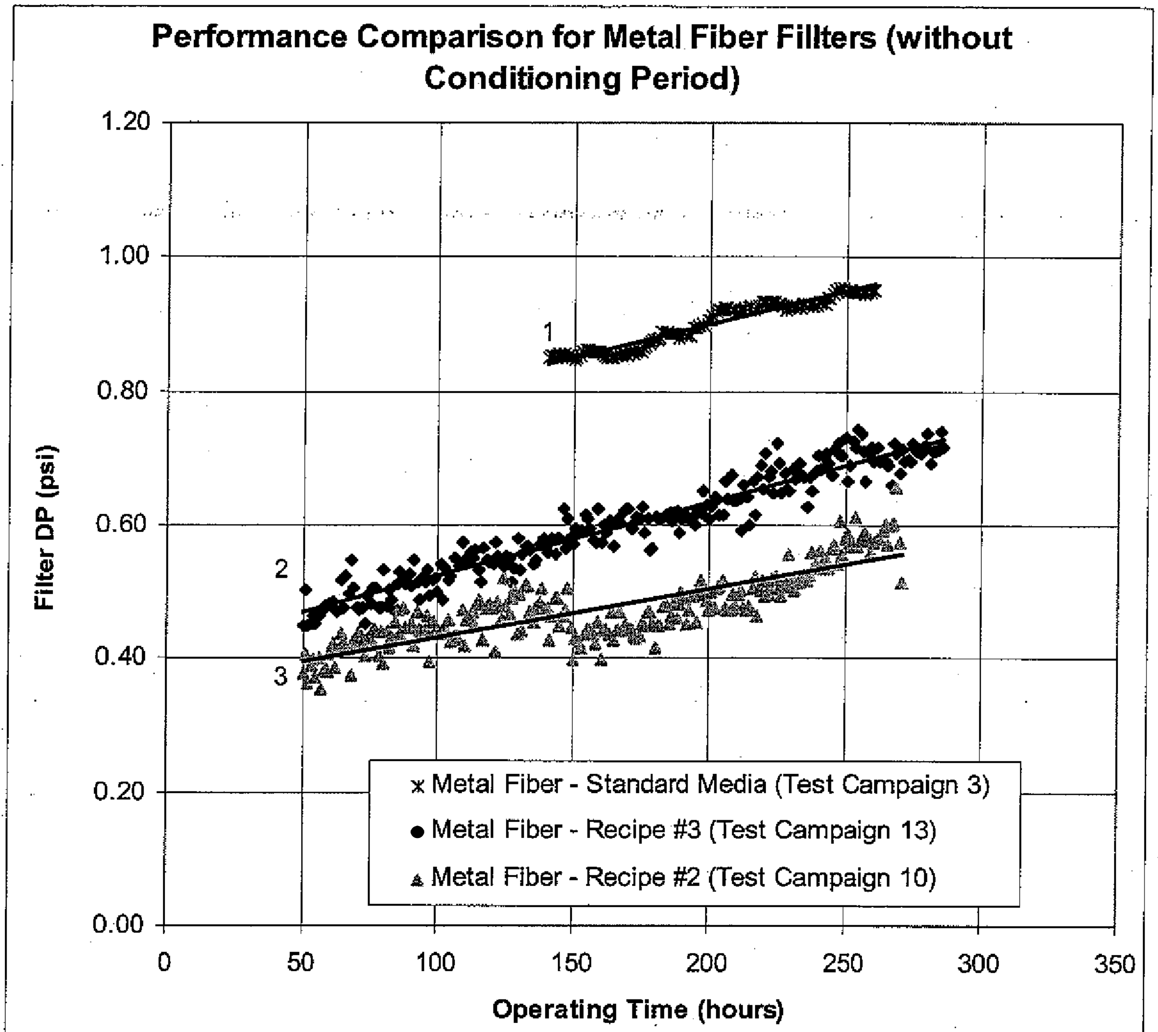

Note: 1. Metal Fiber - Standard Media Predicted Blinding Life = 7780 hours (Test Campaign 3)
2. Metal Fiber - Recipe #3 Predicted Binding Life = 7350 hours (Test Campaign 13)
3. Metal Fiber - Recipe #2 Predicted Binding Life = 10200 hours (Test Campaign 10)

Figure 4.2.14.1: Performance Comparison for Metal Fiber Filters (without Conditioning Period)

4.2.15 Test Campaign 14 (9/8 to 9/13/00)

The fourteenth Slipstream test was structured to support the objectives stated for Test No. 4 in the original test matrix plan (see Table I-1 in Appendix I).

In this test, seven (7) 1.5-meter long metal powder candles were evaluated in the slipstream process. The filters evaluated in Test Campaign 4 were made by the same supplier. The major difference in these filters was a slightly reduced media pore size. Also, these filters had no reduction in the surface pores. The test was planned for 250 hours of syngas operation. The actual test was 114 hours in duration.

There is continued interest in this type of filter construction due to a number of favorable attributes. Inherent to its construction is the ability to withstand higher rates of corrosion. This is a distinct advantage over metal fiber type filters. It costs significantly less to fabricate and is quite robust in the process. This type of filter was used early in the commercial HGF when it was converted from ceramic to metal candles. It offered exceptional corrosion resistance but demonstrated an extremely high rate of blinding.

This study differed from earlier evaluations in that the process syngas was now generated from a petroleum coke gasifier feedstock. The Wabash gasification facility transferred to 100% petroleum coke operation in August of 2000. The main objective in this test was to generate a blinding trend and life prediction for the filter while operating on petroleum coke.

Unfortunately, the study had to be terminated early due to a failure in one of the blowback valves. However, enough data was collected to generate what is believed to be a fairly reliable blinding curve. Figure 4.2.15.1 shows the filter pressure drop as a function of time over the test period. It predicts a blinding life of approximately 236 hours in the process. This is an extremely high rate of blinding when compared to previous trends. This was probably due to increased water loading in the process syngas stream, which is known to cause accelerated rates of filter blinding. However, for reasons not clearly understood, this type of filter is more sensitive to additional water loading in the gas stream. As shown in this study, the blinding rate becomes extremely high. Samples from previous studies were submitted to the filter supplier to examine them for blinding. As in earlier investigations, trace elements (Ge, Sb, As, Pb, etc) were again present in the residual layer and in the candle surface pores. It is theorized that a portion of them condensing in the residual layer are contributing to the loss in permeability. At this time, it still remains unclear how an increase in the gas stream moisture causes this extremely high rate of blinding in the residual char layer.

Due to the inability of these filters to perform acceptably during episodes of small increases in process gas moisture, this type of candle is not considered a good candidate for the Wabash process.

Over the course of this study, there was no appreciable gain in resistance for the backup filter, V-160. For this reason the filtration efficiency for these candles is deemed acceptable for the Wabash gasification process.

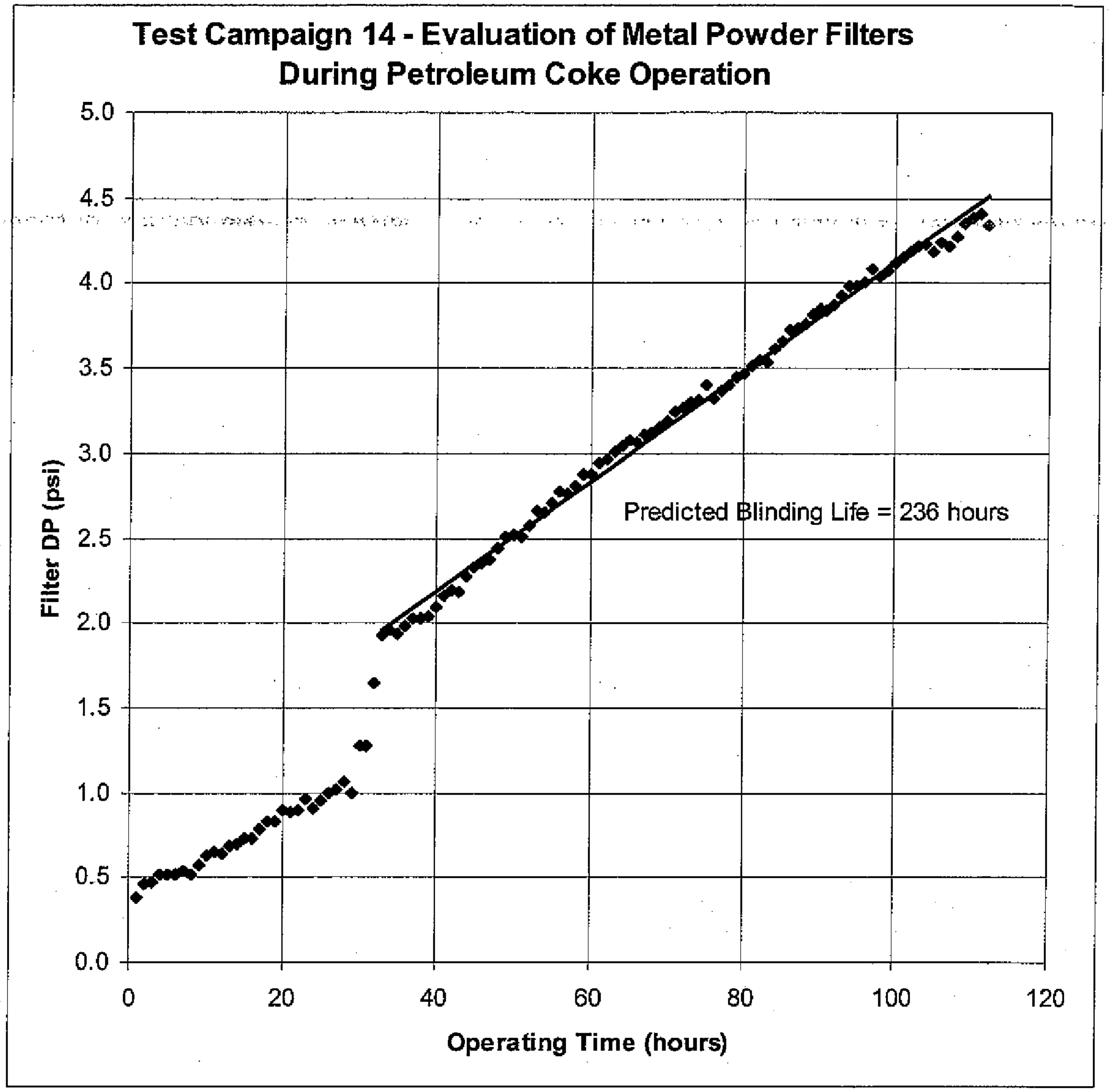

Figure 4.2.15.1: Test Campaign 14 - Evaluation of Metal Powder Filters During Petroleum Coke Operation

4.2.16 Test Campaign 15 (12/11/00)

The fifteenth operating period for the slipstream unit was similar to the first and second campaigns. In this test the gas stream was again isokinetically sampled to determine solids loading in the commercial filters. This study differed in that the gasifier was now operating on a new type of petroleum coke. As in the first test, the data was used to validate process models. Char characterization data was also generated from this sample.

4.2.17 Test Campaign 16 (3/7 to 4/3/01)

The sixteenth Slipstream test was structured to support the development of metal fiber type filters in the Wabash process (see objectives in Section 2.5.1).

In this study seven (7) 1.5-meter long candles containing metal fiber media were evaluated in the slipstream unit. They were constructed the same as filters operated in Test Campaign 10. The filters for this test had 2,347 hours of previous operation in the commercial process. After removal from the HGF, individual candles were subjected to two different cleaning methods to reduce the overall resistance in them. The candles were then installed in the Slipstream for evaluation. The test was planned for 500 hours of syngas operation. The actual test was 620 hours in duration.

Previous studies with this type of filter focused extensively on both corrosion and blinding (see Test Campaigns 8, 10 and 13). Corrosion studies indicate the filters could potentially outlast their blinding life when operated in the commercial process. The life difference becomes even more significant when operating the system with upstream syngas cooler leaks. To address this issue and better optimize filter life, several methods of off-line cleaning were developed to lower process-induced resistance across the filters. Earlier evaluations had shown both methods to be quite effective on other types of candle filters.

The filters for this evaluation had operated in the commercial HGF process and were no longer able to provide another full campaign without reducing their overall resistance. The loss in filter permeability was directly attributable to syngas cooler leaks that developed during this operating time. Consequently, the primary focus was to evaluate filter cleaning efficiency and determine if it would promote corrosion in the filter media. Flow versus pressure drop was measured for the filters before and after cleaning. This data showed a substantial reduction in resistance for both cleaning methods. According to these measurements, the resistance was still 50% higher than a new filter but the overall reduction was significant. Slipstream resistance data at the onset of the campaign were also in agreement with the air flow measurements. Overall, both cleaning methods were found to be quite effective at recovering lost filter permeability.

Another key objective was to develop a blinding trend for the cleaned filters. Figure 4.2.17.1 shows the filter differential pressure as a function of time over the test period. The trend shows a sharp increase in filter resistance for the first 150 or so hours. At this point, the rate of rise is more gradual for the next 200 hours. Following this is an unexplainable sharp increase in resistance for a short period of time until it finally tapers off again. Assuming the first 150 hours of operation is a conditioning period and excluding this data, the blinding trend predicts a filter life of 5,572 hours. If it's assumed that the sharp increase in resistance between 300 and 400 hours of operation is an anomaly, a linear trend can be applied to the last 220 hours of the campaign. The trend is more linear in nature and it predicts a blinding life of 8,415 hours, which is more characteristic of blinding in a metal fiber filter. This prediction would better support the run hours required for filters used in the commercial process. The results demonstrate that cleaning is a viable option to optimize the life of these filters in the Wabash process.

Both cleaning methods require the filters to be submerged in aqueous type solutions. This was somewhat concerning since the media alloy is known to be highly susceptible to aqueous induced corrosion. Consequently, the study also focused on changes in the rate of corrosion that might occur during subsequent filter operation. After 620 hours of slipstream operation pre- and post-test filter specimens were submitted for analysis. An analysis performed by the filter manufacturer determined that both cleaning methods did induce some aqueous forms of corrosion. In fact, one method had caused a significant degree of attack in the candle media. The other caused only a minor penetration into the surface of the fibers in one localized area. There was no indication of accelerated corrosion induced by the process during post-clean operation. The results from this method were encouraging enough to scale up the study to the commercial process.

Over the course of this study, there was no appreciable gain in resistance for the backup filter, V-160. Based on this observation, it was concluded that filtration efficiency was not affected by these cleaning methods.

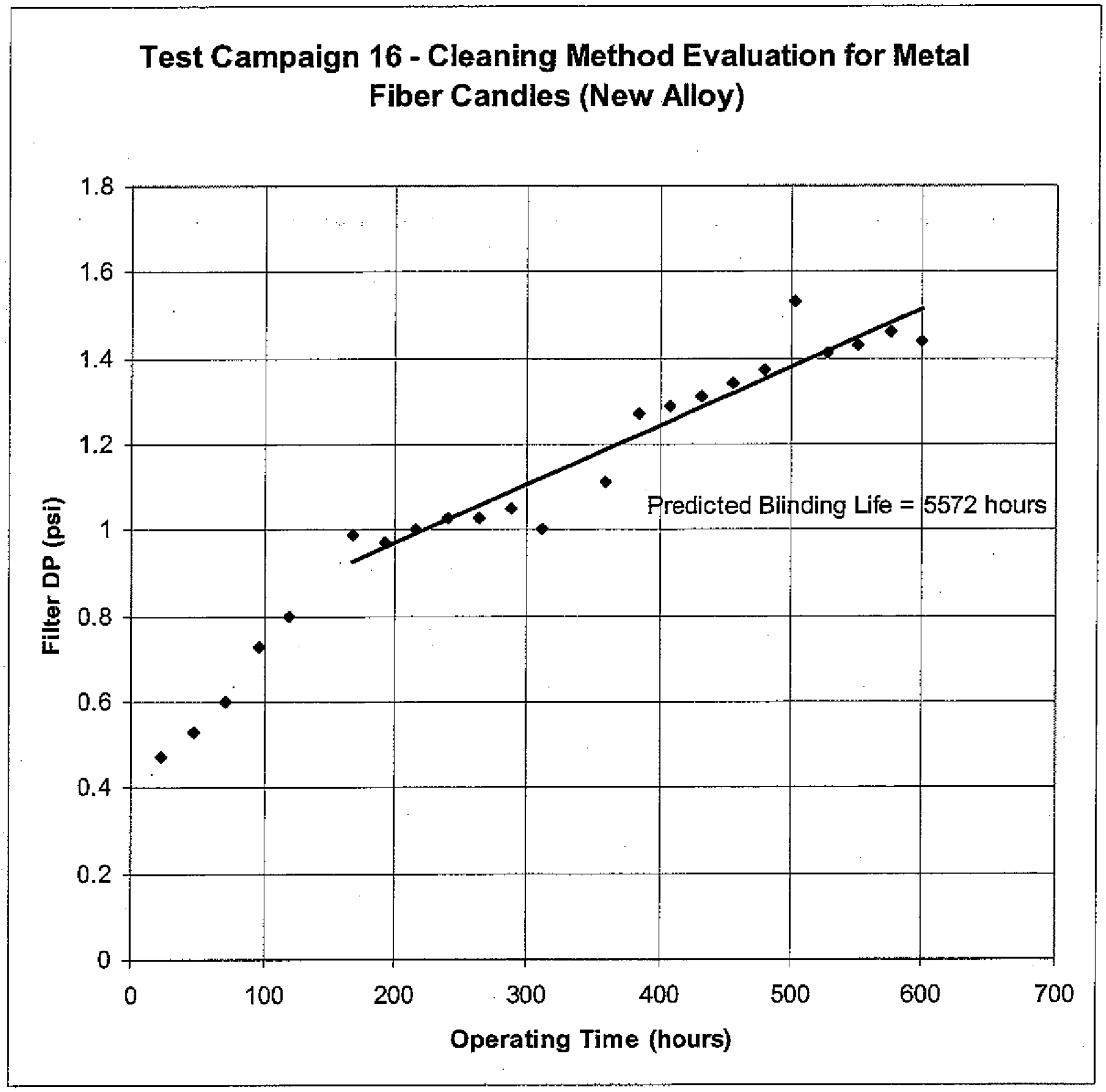

Figure 4.2.17.1: Test Campaign 16 - Cleaning Method Evaluation for Metal Fiber Candles (New Alloy)

4.2.18 Test Campaign 17 (7/14 to 7/21/01)

The seventeenth Slipstream test was structured to support the objectives stated for Test No. 17 in the original test matrix plan (see Table I-1 in Appendix I).

For this test two types of 1.5-meter long oxide composite ceramic filters were evaluated in the slipstream unit. They were obtained from separate manufacturers and both were different from oxide composites evaluated in earlier campaigns. The test was planned for 250 hours of syngas operation. The actual test lasted 188 hours in duration.

In most studies it's undesirable to mix different types of candle filters. Typically, a reliable blinding trend is not established when mixing different types of filters. The major reason for this is the variation in the flow resistance through each filter type. The result is a significant difference in the "instantaneous" face velocity immediately following the blowback cycle. The magnitude of this velocity has a significant affect on the formation and permeability of the residual char layer. This is substantiated by the fact that the permeability of the non-transient layer is directly affected by the blowback event, and more specifically, the force imparted by the high rate of forward flow that occurs immediately thereafter. The high flow causes a greater compaction force in the residual layer that negatively affects its permeability. This can be dramatic for new filters that have the lowest overall flow resistance.

In this case, one supplier could only provide two candles for evaluation so an alternate test plan was needed. The clean resistance of both filters was calculated using air flow versus pressure drop data. The clean resistance in both filters was similar and for this reason it was deemed acceptable that they be tested together. The only caveat to this was that a general blinding rate could only be established for the filters that made up 75% of the vessel loading. To provide additional blinding data, the final resistance was measured for each candle during the post-test evaluation.

Based on results from previous oxide composite studies, the D-158 supply pressure was reduced to 620 psig in an effort to minimize filter damage that might be caused by the blowback gas. Any further reduction might the blowback ineffective at cleaning the candle filters.

The study had to be concluded early due to char leaking through the primary candles. Damage was found in both candles supplied by the one manufacturer. It consisted of multiple areas in which the filtering layer had spalled off of the candle substrate. As in previous studies, it appears that the damage is a result of forces generated in the blowback gas. At the time of this writing the supplier evaluation of the failures is still pending. The other candles suffered no visible damage.

Figure 4.2.18.1 shows the filter differential pressure as a function of time for the test period. The trend yields a predicted life of 3,280 hours. For the five (5) filters tested, this prediction is likely somewhat low. Post-test air flow measurements showed the failed elements had twice the resistance of the others. This high rate of blinding would have negatively influenced the overall trend for the study. It's also difficult to assess how char leakage may have influenced the rate of blinding in all of the candles. Consequently, a new study utilizing only this type of filter (5) is recommended. The operating period should be sufficient to evaluate their robustness in the process.

There was no appreciable gain in V-160 resistance prior to the first 144 hours of the campaign. Based on this data, the filters should provide adequate filtration efficiencies given that the filtering layer remains intact.

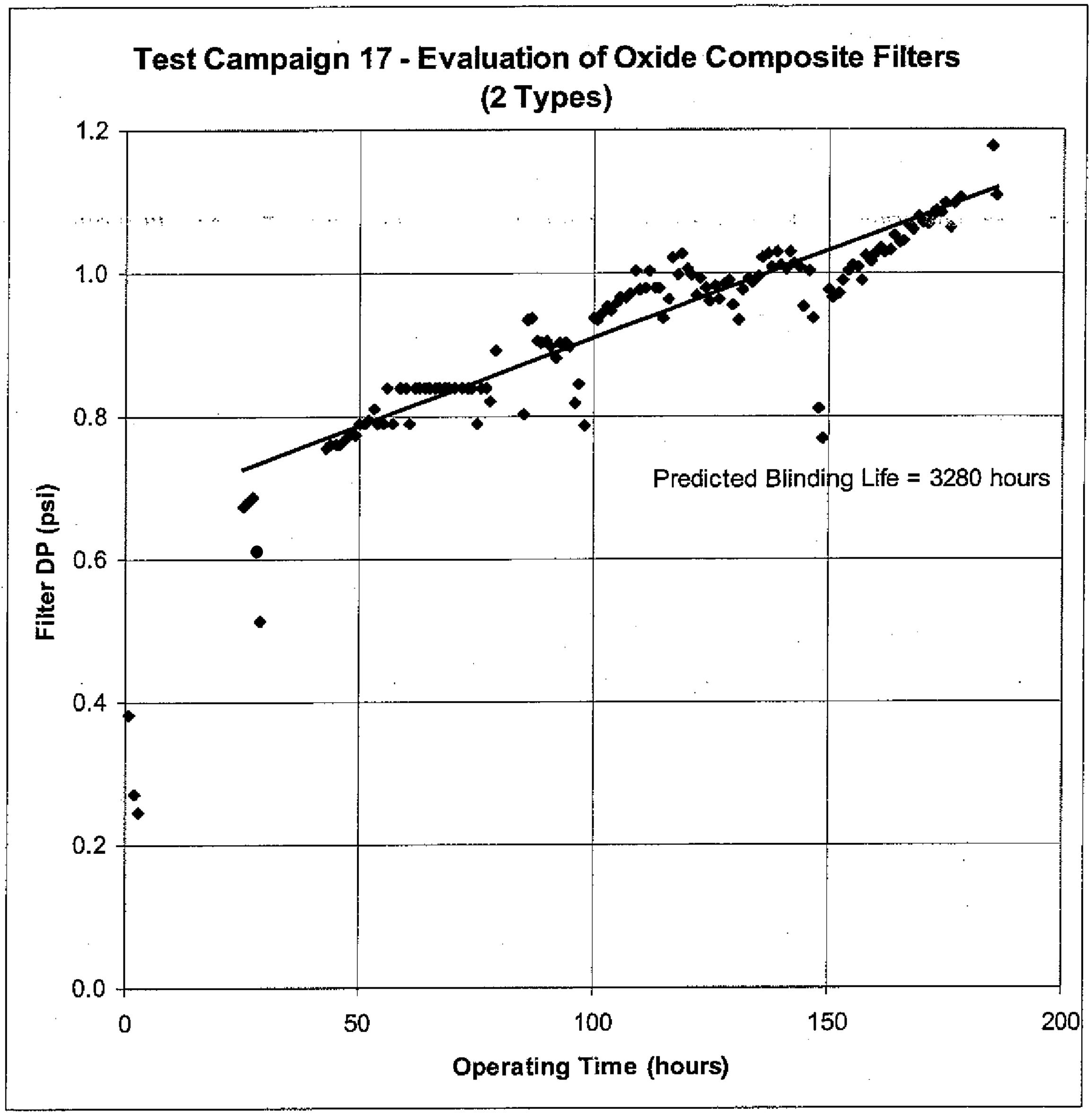

Figure 4.2.18.1: Test Campaign 17 - Evaluation of Oxide Composite Filters (2 Types)

4.2.19 Test Campaign 18 (3/10 to 3/11/03)

The eighteenth Slipstream test was configured to isokinetically sample the incoming syngas to the commercial HGF. The sample was collected with the gasifier operating on petroleum coke feedstock. The data provides a measurement of gas solids loading to compare with various types of gasifier feedstock and for process model validation. A portion of the char sample was submitted to Southern Research Institute for analysis. The data will be used to design a cyclone unit to be operated upstream of the Slipstream system. The study of a cyclone/hot gas filter particulate removal system is being performed under DOE contract DE-PS26-02NT41422-02. Test Campaign 18 was funded by this contract. It has been included in this report as additional slipstream test information.

5.0 CONCLUSIONS AND TECHNICAL INSIGHTS

5.1 Slipstream Validation

Slipstream testing is a valuable tool for predicting filter behavior in the commercial process. Studies involving both metallic powder and fiber elements closely follow commercial HGF trends while operating with similar types of filters. The data trends for larger pore sized clay-bonded silicon carbide filters were similar as well. The agreement in filter behavior between the two systems is validation that the Slipstream is a useful tool to evaluate filters considered for the Wabash HGF process.

5.2 Fail-safe Development

A fail-safe system is a better option to contain char leakage in primary HGF. It provides extremely high HGF reliability and is significantly less costly to operate than a backup filtration system. The fail-safe system in use at the Wabash River facility was originally developed with the Slipstream unit. The fail-safe media will effectively plug and terminate gas flow in a leaking primary filter. Many of the concerns with fail-safe robustness, efficiency, resistance and blinding were addressed in slipstream studies. Longer-term evaluations followed in the commercial process. After operating many fail-safes in excess of 10,000 hours they continue to show little evidence of pore blinding or corrosion. On numerous occasions, the fail-safes have effectively prevented char from leaking into the clean side of the commercial vessels. The devices are so effective that failures are typically concealed until post-filter inspections.

The fail-safe system selected for the Wabash facility has proven highly reliable and is a major reason that the commercial HGF process continues to operate with 100% reliability. It provides extremely low operating and maintenance costs and is highly resistant to both blinding and corrosion in the process.

5.3 Filter Development

The Slipstream was used to support two types of filter programs that are in development at the Wabash facility. One involves finding the optimum metallic filter for the Wabash process and the other is focused on developing a reliable ceramic filter system. This section summarizes the conclusions and technical insights developed during the slipstream test program.

5.3.1 Metallic Filters

For the Wabash process, metal fiber candles offer the highest reliability and lowest operating costs when compared to metallic powder candles. This is primarily due to the lower rate of blinding that occurs in these filters while operating in process. They are less tolerant of corrosion, but by using newly developed alloys, sufficient process life can be achieved (in excess of 8,500 hrs). Some filters still in development indicate that corrosion life could far exceed 10,000 hours.

Most metallic filters are sufficiently constructed (robust) to provide high reliability in the process. Consequently, the two major life limiting factors are blinding (gradual loss of permeability over time) and corrosion. Most corrosion testing was conducted in the commercial HGF because it could easily be structured to minimize plant reliability risk, and offered optimum exposure times. Given this, limited corrosion data is included here. In the Wabash process, metal powder media exhibits a higher resistance to corrosion and a better ability to withstand moderate amounts of corrosion when compared to metal fiber media. It offers an exceptional corrosion life in the Wabash process. This is in part due to the sintering bonds of the metal powder being significantly larger than the fiber diameters of the metal fiber media. It also may have something to do with the manufacturing of the two medias. The metal powder media is annealed after construction and many of the fiber types are not. Residual stresses induced in the fibers as they are drawn may render them more susceptible to corrosion attack. The extremely small diameter of the fibers makes them incapable to withstand what would be considered insignificant rates of corrosion for most other equipment in this industry. Viable candidates for metal fiber candles in the Wabash HGF must be alloys that are virtually impervious to corrosion from the process gas. An extensive test program was used to identify a number of alloys as potential candidates capable of providing sufficient resistance to process induced corrosion. Several of the most promising alloys have operated as test filters and have established corrosion rates predicting a filter life in excess of 10,000 hours. Recently, a number of new alloys have been drawn into media fibers and are in the early stages of the evaluation process. The preliminary results from these alloys are quite promising.

These studies indicate that corrosion is a major concern in metal fiber media when operating in the Wabash HGF process. However, due to recently developed media alloys, several types of metal fiber filters have demonstrated the ability to provide sufficiently high corrosion life, even in gas streams with a hydrogen sulfide content as high as 1.8 %.

Apart from corrosion, the next life-limiting factor for metallic candles is blinding. As stated earlier, blinding is an increasing resistance to flow across the filters during operation. For most candles, the resistance to flow is primarily in the residual char cake that builds on the candle surface. The cake typically extends into the first or second pore layer of the media. Studies indicate that permeability in the residual layer is reduced by a number of factors such as decreasing particle size and a deposition of trace elements within the layer. These can also be influenced by filter differential pressure and blowback frequency.

As mentioned earlier, metal fiber candles provide a lower blinding rate when compared to metal powder candles. Data trends from both the Slipstream and commercial processes have shown metal fiber candles can provide seven (7) times the blinding life of most metal powder filters. The higher void volume and thinner construction of the metal fiber media provides a less torturous path for the blowback gas to travel. This results in higher reverse flow energy available at the candle surface to more effectively regenerate the residual layer. It is believed that the filter typically operates with a thinner residual layer and that it is periodically removed when its resistance becomes sufficiently high. The construction of metal powder filters yields a lower void volume and thicker media resulting in a much more tortuous flow path through the media. This causes a significant pressure drop in the blowback gas resulting in lower reverse flow energy at the candle surface. This has a two-fold effect on filter blinding. First, the higher forward differential pressure drop increases the density of the char layer on the candle surface reducing its permeability. Secondly, the high reverse flow pressure drop renders the blowback energy incapable of "regenerating" any of the non-transient layer. It is believed that this layer becomes thicker and less permeable over time as smaller particles and trace elements migrate into its structure. Data has shown that trace elements strongly adhere to the filter surface and residual char layer as they condense out of the process gas. The combination of char layer densification, increase in thickness, reduction in particle size, and deposition of trace elements all contribute to the high rate of blinding in metal powder media while operating in the Wabash process.

The possible exception to this is the iron aluminide alloy powder candles tested in the slipstream unit. The test data provided a blinding trend comparable to that of most metal fiber candles. However, the iron aluminide candle is incapable of providing an adequate corrosion life in the process. It is interesting to note that the formation of trace element deposits on the outer surface of the iron aluminide filters does not seem to be as significant as in other metal powder media. The trace elements seem to have less of an affinity to form strong bonds to this type of material. In several instances, the residual layer spalled off the outer surface of the filters shortly after removal from the process. This behavior is not totally understood. It was noted that higher cleaning efficiencies (post HGF operation) resulted in the iron aluminide media when compared to filters of similar construction.

Evaluations using SEM/EDS analyses were conducted for metal powder filters previously operated in the Wabash process (coal operation) to determine causes for their high rate of blinding. Results from this study, show a number of trace elements to be deposited on the filter surface and in the residual char layer. The elements found included sodium (Na), magnesium (Mg), aluminum (Al), silicon (Si), sulfur (S), calcium (Ca), iron (Fe), zinc (Zn), germanium (Ge), cadmium (Cd), antimony (Sb), and titanium (Ti) with germanium being most prevalent. Most of these elements were strongly adhered to the particles in the char layer and on the candle surface.

The efficiency of both the metal powder and metal fiber char filters was found to be acceptable for long-term operation in the Wabash process. There has been no evidence of fail-safe blinding or particulate loading in downstream equipment when operating these filter types. Their filtration efficiency was never quantified due to an inability to isokinetically sample the clean gas downstream of the filter system.

5.3.2 Ceramic Filters

One of the most important factors in evaluating ceramic filter reliability is the robustness they demonstrate when operating in the process. In general, there were two types of filters evaluated in this study. They were variations of clay-bonded silicon carbide and oxide composites (CFCC-continuous fiber ceramic composites). Over the course of these studies, the clay-bonded silicon carbide filters demonstrated perfect reliability in the process. In contrast, all but one oxide composite filter failed during operation in the Slipstream system.

The oxide composite filters were stated to have improved toughness in the process due to the continuous fibers used in their construction. For the most part, they demonstrated adequate structural strength during operation. The problem common to all but one oxide composite filter was the low bond strength of the filtering layer. In all filters that suffered damage, there were areas in which the membrane layer looked like it had spalled off during the blowback event. This type of problem persisted even after making significant reductions in the blowback pressure. Based on these results, all but one oxide composite filter was deemed incapable of providing adequate service in the Wabash process. However, the one surviving filter would need to be evaluated for a sustained period of time to determine its ability to resist the same mode of failure. In general, the strength of the filtering layer will need to be improved in these types of candles if they are to provide sufficient robustness in the E-Gas gasification process.

Several types of clay-bonded silicon carbide candles were evaluated in the slipstream unit. Utilizing the proper candle to tubesheet fixing device and bottom restraint system, all filters demonstrated exceptional robustness in the process. The primary focus was then shifted to identifying membranes that offered the best blinding rates. It was generally found that candles with the smallest mean pore size membrane provided the lowest rates of blinding. The vendor specified 5 micron mean pore membrane offered the best overall blinding trend and was found to be as good or better than any of the metallic candles evaluated. The reduced membrane pores had little affect on HGF baseline differential pressure. The 5 micron mean pore membrane was the smallest evaluated in this program. In subsequent studies it was discovered that the rate of blinding in these filters rose significantly for periods where the process syngas moisture was increased slightly above normal levels. The exact reason for this is not clearly understood. Analysis performed on the candles showed that the permeability loss was primarily constrained to the residual layer on the outer surface of the filter. The EDAX analysis again showed high concentrations of germanium within the layer. The residual layer was quite hard, compacted and strongly attached to the membrane material. The structure of this layer had an extremely low porosity. It is still not understood why the additional water vapor in the syngas results in this behavior. This phenomenon also has a negative affect on metallic filter blinding as well. Fortunately the negative affect is less dramatic for metal fiber candles.

For the most part, blinding trends could not be established for oxide composite filters. There was sufficient evidence to show that membrane spalling occurred fairly early in most campaigns and would have negatively influenced blinding behavior.

5.4 Isokinetic Sampling

The Slipstream proved to be a useful system for collecting an isokinetic gas sample of a highly particulate laden process gas stream. The unit was used to sample the syngas just upstream of the commercial HGF. The data obtained from these samples helped validate plant process models for various types of gasifier feedstock. Characterization of the various types of char will be useful for future plant designs. The char is also used in a number of cold flow studies to evaluate alternate filters and filter/cyclone systems.

5.5 Filter Hardware Configurations

One of the more important developments in the ceramic filter studies was a new filter fixing system that held the candle in the tubesheet and restrained its bottom movement. One of the major pitfalls in the original Wabash HGF was that the candles were free hanging. They were fixed at the top within the vessel tubesheet but could swing from side to side at the bottom. Flow induced forces caused the candles to swing and impact each other during process operation. On numerous occasions, the impact was sufficient to spall small pieces (chips) off the bottom of the filters and in some cases resulted in total candle failure (circumferential cracks). A new system was developed to restrain this bottom movement. It is not designed to rigidly hold the candle in place, but effectively restrains it so they can no longer impact each other. Also the system provides additional support that enables the filters to better withstand the negative affects of candle bridging. After Slipstream testing, the new design was successfully evaluated in the commercial HGF. The results have shown it should be a vital part of future ceramic HGF systems considered for the E-Gas process.

A new metallic filter fixing system was developed and tested in the slipstream unit. The system utilizes a new and unique method for fixing the filters and fail-safes within the vessel tubesheet. The new system saves significant time and labor for both the filter installation and removal processes. It also minimizes the risk of damaging filters during assembly. The design facilitates more effective cleaning with the candles fixed in the vessel tube sheets. The new system was purchased for the commercial HGF. Its utilization has yielded significant man-hour and plant downtime savings.

6.0 RECOMMENDATIONS

1. When feasible, slipstream testing should be used to evaluate major process changes. It can accurately predict how changes may affect the process without risking plant production.

2. Slipstream testing at the Wabash facility has been used successfully to improve a number of systems within the process such as hot gas filtration and COS Hydrolysis. When possible, slipstream testing should be used for evaluating all new equipment or major modifications. It provides a low cost way to obtain meaningful data that can accurately predict performance in the process. Slipstream testing can be used to obtain the necessary operating data to ensure high reliability when starting up new equipment.

3. A Slipstream unit is better suited for initial evaluations of materials deemed too risky for testing in the commercial process. However, after the initial evaluation, long-term studies should follow in the commercial process using fail-safes as a filter backup.

4. It's better to conduct filter media corrosion studies in a commercial HGF. It provides the maximum amount of process exposure time, which is often required to obtain meaningful data. Since media corrosion is non-uniform (area specific), and material consumption rates are typically non-linear, it's important to perform these studies over a long period of time (preferably 8,000 hrs or more). Specific procedures defining corrosion analysis methods should be developed and adhered to so that meaningful data comparisons can be made. For coupon testing, the best data is obtained using "flow-through" coupons that are attached to the outer surface of a HGF element.

5. It is recommended that fail-safe devices be used to contain leakage in primary hot gas filters instead of a backup filter system. A properly designed fail-safe system enables the HGF to provide 100% reliability. It's a low capital cost installation and requires minimal maintenance, especially when compared to a backup or secondary hot gas filter.

6. In HGF systems where the potential for blinding is significant, metal fiber or reduced pore membrane SiC ceramic filters should be considered.

7. Filters that develop high resistance during operation can typically be removed from the process and cleaned using a hot aqueous solution. There are numerous methods commercially available. Evaluations should be made to determine cleaning efficiency and negative effects that might be induced by the process.

8. HGF slipstream vessels should be designed with ample clean side plenum space to incorporate testing of various fail-safe devices. The Wabash slipstream vessel had sufficient clean side volume for this testing but it did require some modifications to the blowback system.

9. Include redundant instrumentation for key operating parameters in the original design of a slipstream system. This is necessary to prevent losing critical operating data should an instrument problem develop.

10. Alarms should be incorporated into DCS control code to alert operations in the event of key operating parameter instrumentation failure. This should be considered for each instrument deemed impractical for redundancy. Detailed instructions should be provided to operations personnel that describe corrective actions to be taken when addressing these alarms.

11. Temperature indication should be included downstream of slipstream pressure relief devices. This along with vessel pressure indication can alert the operator of a lifting relief device. PSV relief indications, specifically pressure and temperature (temperature is less costly than flow indication), should be used to transfer the system into a safe shutdown mode. Downstream temperature measurement can also detect if the PSV properly reseats. This prevents erosion damage to the PSV from solids laden gas flowing through the device. Furthermore, critical DCS instrumentation and equipment should be

programmed such that it cannot be placed in manual control without using the proper system interlocks.

12. All syngas and solids transport lines should have adequate nitrogen purge capabilities. All lines should be purged of syngas during the shutdown process. This is especially important for the solids transport line to prevent plugging problems that can occur after the system is cooled down.

13. All slipstream piping and equipment should be heat traced with a system designed to maintain normal process operating temperatures. It is important to maintain the slipstream process at commercial operating temperatures to obtain meaningful data.

14. All filter element supplier QA/QC manufacturing programs should be audited thoroughly, and if necessary, customized by the buyer specifically to ensure they meet plant HGF reliability goals. In setting up a filter element QA/QC program, the supplier should fully understand the performance requirements of the customer's system. This was required several times to address manufacturing defects in filters and fail-safe devices tested at the Wabash facility.

15. Bottom restraint systems should be used to enhance the reliability of HGF systems that use free-hanging ceramic candles. Restraining filter bottom movement not only prevents damage from swinging candles impacting each other, it also helps prevent headpiece gasket attrition that can result from this type of movement. This system also renders candles much more capable of withstanding forces generated by solids bridging.

16. Continue fail-safe development for ceramic filters. Fail-safes are an integral part of a highly reliable ceramic HGF. A number of conceptual fail-safes designed to contain leakage in both the candle and candle gasket have been developed. The new designs should be evaluated for effectiveness in a slipstream process prior to using them in a commercial HGF.

17. Additional blinding and corrosion studies should be conducted for higher chromium iron aluminide powder filter media.

18. Conduct additional research to determine why slight increases in syngas moisture can accelerate the rate of filter blinding.

19. Perform additional blinding studies on the newly developed thin-walled metal powder media filters.

REFERENCES:

Alvin, M. A., 1996. Westinghouse Electric Corp., Unpublished results from evaluation of Destec Gasifier exposed metal and ceramic filters.

Boxall, I., Cook, A. P., 1997 – 2001. Fairey Microfiltrex Ltd., Unpublished results from appraisal of filter media samples operated in the WREL gasification process.

June, M.R., 1998. Pall Advanced Separation Systems, Unpublished results from evaluations of metal powder filters operated in the WREL gasification process.

June, M. R., 2000. U. S. Filter, Unpublished results from filter media alloy evaluations in the WREL gasification process.

Seymour, P. T., 1996. Schumacher Filters America, Inc., Unpublished results from SEM analysis of blinding in DIA-SCHUMALITH filters.

Walch, A., 2000. USF Schumacher, Unpublished results from examination of a DIA-SCHUMALITH candle operated in the WREL gasification process.

McKamey, C. G., Tortorelli, P. F., Lara-Curzio, E., 2001. Oak Ridge National Laboratory, Unpublished results from examination of iron aluminide hot gas filters operated in the WREL gasification process.

Coyle, J., 1995 – 1999. Dynegy Power Corp., Unpublished results from evaluation of various metal filters exposed to the WREL gasification process.

Merrick, D. D., 1995 - 1997. Dow Chemical Co., Unpublished results from cold flow particulate filter evaluations.

Appendix I

Listed below in Table 2.5.5.1 is the original test matrix that was submitted in Task 3 of the Test Plan for D.O.E. award number DE-FC26-97FT34158. The actual matrix that made up the Slipstream test program is listed as Table 2.4.5.1 in this report. Deviation from the original test plan was necessitated to better optimize plant HGF reliability and maintenance.

Table I-1 Original Proposed Slipstream Test Matrix

Meets Obj. #	Test No.	Filter Type	Test Description	Test Duration	Operating Parameters	Test Qty.
7	1	Sintered Woven Metal Fiber (13 micron mean pore)	Perform isokinetic sampling utilizing DCSS unit. Calculate particulate loading to commercial scale h ot gas filter vessels.	10 hrs	Refer to Sec. 3.4	2
1,2,3,8	2	Sintered Metal Fiber Type Filters (13 micron mean pore) with Sintered Metal Powder Safety Fuses (20 micron mean pore)	Perform blinding study and compare to plant data. Evaluate filter efficiency effects on fuse plug permeability. Estimate filter life in full scale system.	250 hrs	Refer to Sec. 3.4	1
1,2,3	3	Sintered Metal Powder Filter (20 micron mean pore)	Perform blinding study on filters and compare to plant and DCSS test data. Estimate filter life in full scale system.	250 hrs	Refer to Sec. 3.4	1
1,2,3	4	Sintered Metal Powder (13 micron mean pore)	Perform blinding study on filters and compare to plant and DCSS test data.	250 hrs	Refer to Sec. 3.4	1
1,2,3	5	Sintered Metal Powder (calandered media)	Perform blinding study on filters and compare to plant and DCSS test data. Estimate filter life in full scale system.	250 hrs	Refer to Sec. 3.4	1
1,2,3,6	6	Ceramic Competitor A (5 micron mean pore membrane)	Perform blinding study on filters and compare to plant and DCSS test data. Estimate filter life in full scale system.	250 hrs	Refer to Sec. 3.4	1
1,2,3,6	7	Ceramic Competitor B (5 micron mean pore membrane)	Perform blinding study on filters and compare to plant and DCSS test data. Estimate filter life in full scale system.	250 hrs	Refer to Sec. 3.4	1
1,2,3,6	8	Ceramic Competitor B (15 micron mean pore membrane)	Perform blinding study on filters and compare to plant and DCSS test data. Estimat e filter life in full scale system.	250 hrs	Refer to Sec. 3.4	1
1,2,3	9	Sintered Woven Metal Fiber (13 micron mean pore with modified filter media fixing)	Test filter in tegrity/efficiency. Consider using safety fuses.	250 hrs	Refer to Sec. 3.4	1
1,2,3	10	Sintered Woven Metal Fiber (13 micron mean pore with modified support structure)	Test filter in tegrity/efficiency. Consider using safety fuses.	250 hrs	Refer to Sec. 3.4	1
3	11	Sintered Metal Powder (13 micron mean pore)	Perform candle filter pre-conditioning studies. Compare blinding rates to plant and DCSS test data.	250 hrs	Refer to Sec. 3.4	1
3	12	Sintered Metal Powder (13 micron mean pore)	Quench incoming solids laden gas and evaluate effects on blinding rates. Compare to previous DCSS test data.	250 hrs	Refer to Sec. 3.4 except for lower operating temperatures.*	1
3,4	13	Sintered Metal Powder (13 micron mean pore)	Study the effects on filter blinding rates while varying backpulse frequencies.	500 hrs	Refer to Sec. 3.4 except for backpulse cycle time.*	1
3	14	Sintered Metal Powder (13 micron mean pore)	Increase/decrease backpulse gas temperatures to evaluate effects on filter blinding. Compare to baseline DCSS test data.	500 hrs	Refer to Sec. 3.4	1
4	15	Sintered Metal Powder (13 micron mean pore)	Perform backpulse gas optimizatio n studies.	500 hrs	Refer to Sec. 3.4 except for backpulse gas pressures.	1

3,9	16	Sintered Metal Powder (13 micron mean pore)	Introduce slurry quench in gas side stream taken off upstream of high temperature recovery unit and evaluate effects on filter performance. Also study effects on gas composition and solids loading.	1000 hrs	Operating parameters will be specified prior to initiating this test.	1
1,2	17	Ceramic Composite Type	Perform blinding /integrity studies. Compare to baseline DCSS test data. Evaluate filter material strength.	250 hrs	Refer to Sec. 3.4	1
1,2	18	Ceramic Membrane Covered Monolithic Type	Evaluate performance (blinding rate, efficiency, etc.) as a primary filter.	250 hrs	Refer to Sec. 3.4	1
5,9	19	Sintered Metal Powder (13 micron mean pore)	Test up flow gas distribution system. Evaluate filter performance with this configuration.	250 hrs	Refer to Sec. 3.4	1
5,9	20	Sintered Metal Powder (13 micron mean pore)	Evaluate maximum filter gas impingement velocities. Results will be useful for internal gas distributor design.	500 hrs	Refer to Sec. 3.4	1
9	21	Ceramic Competitor A or B(5 micron mean pore membrane)	Test multi-tiered filter configuration (LLB design).	1000 hrs	Refer to Sec. 3.4	1

*Modified operating parameters will be specified prior to initiating this test.

APPENDIX II

Characterization of Field-Exposed Iron Aluminide Hot Gas Filters

Claudette G. McKamey
Metals and Ceramics Division
Oak Ridge National Laboratory
P.O. Box 2008, MS-6115
Oak Ridge, TN 37831
Ph. 865-574-6917
Fax 865-574-7659
mckameycg@ornl.gov

Peter F. Tortorelli
Metals and Ceramics Division
Oak Ridge National Laboratory
P.O. Box 2008, MS-6156
Oak Ridge, TN 37831
Ph. 865-574-5119
Fax 865-241-0215
tortorellipf@ornl.gov

Edgar Lara-Curzio
Metals and Ceramics Division
Oak Ridge National Laboratory
P.O. Box 2008, MS-6069
Oak Ridge, TN 37831
Ph. 865-574-1749
Fax 865-574-6098
laracurzioe@ornl.gov

David McCleary
Global Energy Inc.
444 West Sanford Ave.
West Terre Haute, IN 47885
Ph. 812-535-6097
Fax 812-535-6100
dpmccleary@GlobalEnergyInc.com

John Sawyer
Pall Process Equipment Development
3669 State Route 281
Cortland, NY 13045
Ph. 607-753-6041
Fax 607-753-8525
John_Sawyer@Pall.com

Roddie R. Judkins
Fossil Energy Program
Oak Ridge National Laboratory
P.O. Box 2008, MS-6084
Oak Ridge, TN 37831
Ph. 865-574-4572
Fax 865-574-4357
judkinsrr@ornl.gov

Characterization of Field-Exposed Iron Aluminide Hot Gas Filters

Keywords: hot gas filters, iron aluminides, microstructural analysis, mechanical strength

Introduction

The use of a power turbine fired with coal-derived synthesis gas will require some form of gas cleaning in order to protect turbine and downstream components from degradation by erosion, corrosion, or deposition. Hot-gas filtration is one form of cleaning that offers the ability to remove particles from the gases produced by gasification processes without having to substantially cool and, possibly, reheat them before their introduction into the turbine. This technology depends critically on materials durability and reliability, which have been the subject of study for a number of years (see, for example, Alvin 1997, Nieminen et al. 1996, Oakey et al. 1997, Quick and Weber 1995, Tortorelli, et al. 1999).

Materials used in hot-gas filters are required to withstand prolonged exposure to corrosive, high-temperature gaseous environments, as well as to condensable vapors and solid species, some of which may have the potential for localized interaction with the filter material after extended times. The gas streams may be purely oxidizing (such as those produced by pressurized fluidized bed combustors, PFBCs) or relatively reducing, in which the sulfur species are principally in the form of H_2S, as in the case of the product gas from integrated gasification combined cycle (IGCC) processes or from carbonizers. Degradation of metallic filter elements has been observed under oxidizing, sulfidizing, and/or carburizing conditions and acts as a driving force for the development of ceramic hot-gas filters, particularly for the higher temperatures associated with advanced gasification and combustion designs. However, iron aluminides can also be considered for such applications because they offer reliability advantages over ceramic filters and typically have good to exceptional high-temperature corrosion resistance in a variety of sulfur-bearing environments relevant to coal-derived energy production systems (DeVan 1989, McKamey et al. 1991, DeVan and Tortorelli 1993, Tortorelli and DeVan 1996, Gesmundo et al. 1994, Natesan and Tortorelli 1997, Blough and Seitz 1997, Saunders et al. 1997a, Bakker 1998).

Metallurgical and mechanical evaluations of porous Fe_3Al-based alloys exposed in test beds that simulate environments associated with IGCCs and PFBCs have been conducted (Tortorelli et al. 1998, Tortorelli et al. 1999). Results for as-fabricated porous iron-aluminide filter materials showed good high-temperature corrosion resistance in air, air + SO_2, and H_2S-containing environments. The corrosion resistance was further improved by a preoxidation treatment. The hoop strength of the filters was not significantly affected by the preoxidation treatment or by 100-h exposures in air or air plus SO_2 at 800 and 900°C. The purpose of the current study was to extend such evaluations to iron-aluminide filters that have been exposed in an actual gasification plant. As described below, iron-aluminide filters showed good performance under plant conditions when preoxidation was effective in establishing a thin, protective surface alumina.

Experimental Procedures

Sintered iron aluminide filter elements have been used for hot-gas cleaning at Global Energy Inc.'s Wabash River (Indiana) gasification plant. These cylindrical (~58 mm outer diameter, 2 mm wall thickness) elements were fabricated by Pall Corporation (Cortland, NY) from water-atomized alloy powder produced by Ametek Specialty Metals Division (Eighty-Four, PA). The composition of the powder was nominally Fe-28 at. % Al-2% Cr-0.1% Zr (FAS-Zr). Several pieces of FAS-Zr elements were supplied by Global Energy, Inc. to Oak Ridge National Laboratory after use in the Wabash River Plant's clean-up system. In other cases, o-ring specimens (width of approximately 12.7 mm) were cut from as-fabricated Pall elements, inserted into the filter system at Wabash River for various lengths of operating time, and then returned to ORNL for evaluation. (The general exposure conditions are listed in Table I.) The elements from which the specimens were cut were usually fabricated of FAS-Zr, but in a few cases, o-rings of an FAL alloy composition (Fe-28 at.% Al-5% Cr-0.1% Zr) were exposed. During these exposures, the filter materials were exposed to gas produced by combustion of either coal or petroleum coke at temperatures estimated to be in the range of 450-500°C (see Table I). Note that, in the case of the o-rings, specimens were either placed directly in the filter vessel (dirty-gas side) or in the plenum that routes the filtered gas from the element bundles (clean-gas side).

Evaluation of filter materials included mechanical testing of o-rings by internal pressurization to determine tangential (hoop) stress-strain behavior. The o-rings tested in this manner were from the specimens exposed as such (see above) or were cut from the pieces of actual filter elements received from the Wabash River plant. The internal pressurization tests were conducted in ambient air either by subjecting an elastomeric insert (for as-fabricated filter samples) to axial compression at a constant displacement rate of 2 mm/min or by use of a positive radial-displacement wedge mechanism (for the field-exposed filter samples) (Lara-Curzio 1999). After mechanical testing, the fracture surfaces were examined using scanning electron microscopy (SEM) and pieces were cut from the o-rings for microstructural analysis using optical and SEM, energy dispersive x-ray spectroscopy (EDS), electron microprobe, and Auger electron spectroscopy.

Results

As-fabricated Filter Materials

The as-fabricated filter materials were examined by quantitative image analysis of polished sections. It was determined that they were 40-50% porous with sintered ligaments that ranged between 1 and 30 μm in thickness with a mean value of approximately 9 μm. There were numerous oxide particles on pore surfaces (Fig. 1) and at the boundaries of agglomerated powder particles (Tortorelli et al. 1998). Qualitative analysis by EDS showed that these particles were most likely alumina and zirconia. These oxides form during the water atomization process and most likely coarsened during subsequent processing. After preoxidation at 800-1000°C, the original oxide particles were still clearly evident and a thin protective alumina scale had formed on the metal surfaces. (Pall typically preoxidizes the iron-aluminide filter elements.) Depth profiling by Auger electron spectroscopy showed that the alumina scale formed by preoxidation at 800°C averaged approximately 2 μm in thickness, but could vary between 0.5 and 3 μm. Filters with oxide layers in this thickness range were gray in color. A filter element with various shades of blue also was used to provide o-ring specimens for exposure at the Wabash River Plant. This coloration would indicate a thinner alumina film was formed during preoxidation and, indeed, Auger analysis determined that the oxide coating on the pore surfaces of the blue filter was approximately 0.2 μm. An as-fabricated filter without preoxidation was similarly analyzed and was found to have an alumina layer that was no more than several hundredths of a micron thick.

Determination of the room-temperature tangential stress-tangential strain curves using the elastomeric-insert-internal pressurization approach showed that, when allowance is made for the reduced load-bearing area, the measured strengths of the porous iron aluminides appear to be consistent with those for similar dense alloys (McKamey et al. 1991). The average fracture strength for o-rings cut from two as-fabricated filter elements (IA-187, IA-188, three specimens each) was approximately 2 kN (Table I). Microscopy of the ruptured o-rings showed that failure was transgranular through the fully sintered ligaments and the fracture surfaces were free of oxide particles (Fig. 1). As such, the fracture surfaces were typical of the ductile failures observed for fully dense iron aluminide (McKamey et al. 1991). Preoxidation at 800°C for 7 h had no influence on the hoop strength of the FAS-Zr filter material (Tortorelli et al. 1998).

Specimens from Exposed Filter Elements

Two different samples of the DC-20 filter, exposed for 574 h in the filter vessel at the Wabash River plant, were examined (Table I). The porosity in this filter was non-uniform, with the sample in Fig. 2a showing normal porosity, while the sample in Fig. 2b had less porosity over the inner half of the filter. A light deposit containing S, As, Ge, Si, Cu, Sb, C, Zn, Ca, K, P was observed on the outer surface (that is, the gas inlet side of the filter wall) of both samples. Very little deposit was present on the inner (gas outlet) surface.

The DC-36 filter saw the same exposure conditions as the DC-20 filter, but for a longer time (1565 h). The porosity in this filter was non-uniform, with the inner one-third of the filter having much less porosity than normal (like that shown for DC-20 in Fig. 2b). The outer surface of the filter (at the top in Fig. 2b) contained a light-to-medium deposit consisting of As, Ge, S, Si, and O, while the inner surface had a very light deposit of mostly S and C. Pore surfaces in the interior of the filter were covered with an Al-O product approximately 2 μm thick. Corrosion due to the exposure was not substantial.

Filter element DC-88 was exposed in the vessel at Wabash River for 2185 h. As shown in Fig. 3, microstructural examination indicated that many of the pores in approximately the outer 750 μm of the filter (top in Fig. 3), as well as approximately 300 μm from the inner surface, were almost completely filled. In addition, layers of corrosion products approximately 100 and 50 μm thick were observed on the outer and inner surfaces, respectively. These layers appeared to be growing outward from the filter, since the wall thickness after exposure was about 200 μm greater than before exposure. The fracture strength of this filter element, along with that of DC-36 above, was less than that of the DC-20 and as-fabricated filters (see Table I).

The microstructure and composition of the DC-88 filter element after exposure was characterized using an electron microprobe. Figure 4 shows that the occluded filter region near the outer surface was composed of basically two phases: an Al/Cr-based oxide (see Figs. 4c,f) and an Fe-based sulfide (see Figs. 4b,e). The layer that formed outward from the surface was Fe-S. No areas of Fe_3Al were detected in this 750-μm region near the outer surface, indicating that the entire original Fe-Al-Cr matrix in this area had been consumed by corrosion. The Cr in the original filter material appears to have been incorporated predominantly into the oxide phase (see Fig. 4d). Microprobe analysis showed that the Fe-S layer on the surface also contained many other elements and particles filtered from the gas stream, including oxides of Al and Si, as well as Ni, Zn, Ca, K, Ge, As, and Sb. The occluded region of the inner surface (that is, the outlet side of the filter wall) was also composed of Fe-S and an Al/Cr-based oxide, with a surface layer of Fe-S. The layer also contained a significant amount of As and some Ni, but few, if any, of the other elements that were observed on the outer surface. In the transition regions of the filter, between the completely occluded regions and the porous original matrix still present toward the center of the filter, some of the Fe-Al-Cr matrix phase was detected along with the Fe-S and oxide phases. Figure 5 shows a micrograph and an x-ray scan taken across such a region. The x-ray data revealed the light and medium contrast phases to be Fe-Al-Cr and Fe-S, respectively. The composition of the Fe-Al-Cr phase shown in the x-ray scan is approximately the same as the original filter material, (i.e. Fe-28Al-2Cr), while the composition of the Fe-S phase indicates that it is most likely FeS. A spike in the Al and O levels and a decrease in the Fe level at the interface between these two phases indicate that an oxide layer is still present on the surface of the Fe-Al-Cr particle; presumably it is the Al_2O_3 layer produced by preoxidation. The dark phase is a complex oxide containing Fe, Al, S, and Cr. The layered structure of that phase shown in Fig. 5a and the composition shown in Fig. 5b suggest that it may be an intermediate phase between the Fe-Al-Cr matrix and the FeS/oxide structure present nearer the outer and inner surfaces of the filter.

Specimens Exposed as O-rings

As described in the Experimental Procedures section, o-ring specimens were cut from as-fabricated filter elements and then exposed on the clean- or dirty-gas side of the Wabash River Plant's filtration system. Three o-rings were exposed on the clean-gas side of the filter system without preoxidation: IA-188 for 1628 h, IA-187 for 2237 h and another o-ring of IA-187 for 3865 h. Figure 6 compares the microstructures of these three filter o-rings after exposure. All three o-rings appeared to be blocked with reaction products, with only a small percentage of the pores open toward the outer and inner surfaces of the filter exposed for 1628 h. Higher magnification of the center areas of these filters shows the presence of three main phases (the three levels of contrast in Fig. 7), with the lighter contrast phase (the Fe-Al-Cr matrix) gradually disappearing with time. Analysis of these three phases using EDS showed that, with continued exposure, the Fe-Al-Cr matrix was gradually being converted into oxide and Fe-S products (the dark and medium contrast phases, respectively, in Fig. 7). Higher magnification SEM (Fig. 8) and EDS showed that heavy elements in the coal gas (e.g., As, Ge, Sb) tend to become trapped in the Fe-S phase. For example, the very bright spots in Fig. 8 are particles of As in the Fe-S phase. The results of internal pressurization tests of o-rings from the IA-187 filter exposed for 2237 h showed that the strength was reduced by approximately half in comparison to the as-fabricated filters (Table I).

O-rings from filter elements that had been preoxidized for 7 h at 800°C were exposed on the clean-gas side of the filter system (Table I): DC-207 for 1988 h, IA-191 for 2237 h, and DC-205 for 4335 h. The o-rings exposed for 2237 and 4335 h were in very good condition, with no surface deposits, no reduction in strength, and only minor Fe-S formation throughout the filter. Their microstructures were similar to that observed for the typical unexposed filter (as in Fig. 2a). However, gas flow in the DC-207 o-ring, which had been exposed for only 1988 h, was completely blocked by the formation of almost solid bands of corrosion products on the outside and inside surfaces (see Fig. 9), in addition to corrosion products scattered throughout the interior of the filter (Fig. 10). High magnification SEM (Fig. 9b) and EDS (Fig. 9c) indicated again that the Fe-Al matrix was being converted into Fe-S and oxide products. These results and the results of other analyses discussed above suggest that the iron diffuses outward to fill the pores with Fe-S, a conclusion that has also been reached by others (Bakker and Stringer 1997). The corrosion products formed throughout the thickness of the filter and Fig. 10 shows the Fe-S growing inside the pores in the center of the DC-207 filter.

As part of the study of preoxidation conditions, two o-rings (from filter IA-141) that were preoxidized at 1000°C were exposed for 2237 and 3865 h on the clean-gas side of the plant's filtration system. The microstructures of the o-rings exposed for 2237 and 3865 h were similar to those shown in Fig. 6a,b. Both o-rings appeared to be blocked to the flow of gas although the one exposed for

2237 h still had a noticeable number of unblocked pores. Each had layers of Fe-S on both surfaces, the thickness of which approached 100 μm. High magnification SEM showed an increase in corrosion products and a decrease in the amount of Fe-Al matrix with increasing exposure time, as was shown for the as-fabricated filters in Fig. 7.

As described above, a filter element with a thinner (blue) preformed oxide layer on pore surfaces was used to provide o-ring specimens for exposure at the Wabash River plant. After plant exposure for 1988 h, the o-rings cut from the blue filter (o-rings DC-208 and -211 in Table I) contained only small amounts of corrosion product regardless of location on the clean- or dirty-gas side and their microstructures were similar to that of the as-fabricated filter shown in Fig. 2a. In contrast, o-rings from the gray preoxidized filters exposed at the same time for the same length of time (o-rings DC-209, -210 in Table I) were almost completely blocked by the formation of Fe-S and oxide products (Fig. 11). The presence of such a large amount of the more brittle corrosion products resulted in significantly reduced fracture strengths for the gray o-ring specimens (0.9-1.5 kN, Table I).

Four FAL (see Experimental Procedures section) o-rings were included in the various exposures at the Wabash River Plant and the results are listed at the end of Table I. All the exposed FAL o-rings, whether exposed for 6212 h on the clean-gas side or for 4335 h on the dirty-gas side, exhibited minimal amounts of corrosion products. As expected, the surface deposits on the o-rings exposed on the dirty-gas side were much thicker than on the o-rings exposed on the clean-gas side, but this thicker surface deposit did not affect the appearance, strength (Table I), or filtering capacity of the FAL o-rings.

Strength Measurements

Examination of the strength data reported in Table I indicates an inverse correlation between the amount of sulfidation observed and the fracture stress of the o-ring during loading by internal pressurization. The hoop-strength data, albeit limited, when combined with the microstructural analyses, qualitatively indicate that the iron-aluminide filters maintain approximately their original strength as long as Fe-S formation has not occluded more than approximately 50% of the pores.

Discussion

Evaluation of specimens from plant exposures is complicated by variations in operating conditions from one run to another. Both coal and petroleum coke (higher sulfur content) were used as fuel during the exposure sequences and the temperature was not necessarily the same in each run (probably ranged between 450 and 550°C). In addition, many of the longer exposure times were actually made up of as many as three different campaigns between which the specimens were exposed to unknown lengths of downtime and any possible corrosion associated with such (Bakker 1998, Bakker and Stringer 1997, Saunders et al. 1997b). Nevertheless, this work has yielded some important information about the nature of corrosion of iron aluminides in an operating gasification plant and the effects of composition and preoxidation.

Iron aluminide alloys rely on a thin alumina scale for protection against corrosive environments at high temperatures. For this application, filter elements are normally preoxidized at temperatures much higher than the gasification filtration unit to assure that a protective alumina film forms. This scale has been observed on preoxidized elements (see above and Tortorelli et al. 1998). In this work, o-ring specimens cut from filters that were not preoxidized and from an element preoxidized at 1000°C were found to be fairly heavily corroded after as little as 1628 h of exposure (see results for IA-141, -187 and -188 in Table I and Figs. 6-8). In contrast, with one exception (DC-207), the o–rings preoxidized at 800°C were still not filled with corrosion products after 4335 h (see results for IA-191, DC-205, -207 in Table I and Fig. 9). Even in the case of DC-207, corrosion was not as severe as in the absence of preoxidation; its fracture strength (which generally tended to decrease with increasing corrosion – see Table I) was equal to the starting material. These results show the importance of the formation of a continuous alumina layer in assuring corrosion resistance during operation of the gasifier and reinforce the need for appropriate and reproducible preoxidation in this regard. [Presumably, the poorer performance of actual filter elements used in the early phases of this study (e.g., DC-88) may have been due to nonoptimal preoxidation.] Preoxidation at 1000°C was not as effective as that done at 800°C. In another study (Pint 2000), the 1000°C preoxidation treatment was found to result in an alumina layer on the filter that was locally disrupted by large zirconia particles and not uniformly continuous and thin. Because of this (and Al depletion concerns – see below), it would not be expected to be as protective as the one formed by preoxidation at 800°C.

Corrosion failure in these filter materials appeared to be associated with the formation of Fe-S inside the pores of the filter. This may mean that sulfidation is kinetically favored under thse exposure conditions. However, as described above, Al-containing oxide products were always observed in conjunction with the sulfides. This observation is consistent with a type of breakaway oxidation (sulfidation) in which aluminum is locally depleted by growth of alumina so that, after some point, if the protective scale is breached, iron sulfides form relatively rapidly. The thinness of the ligaments of the filters (mean diameter of 9 μm) magnifies the importance of aluminum depletion/breakaway as the degradation mode because there is a relatively small volume of this element available to form the protective alumina (Quadakkers and Bongartz 1994). This suggested mechanism can explain the better performance of the blue filter materials vis-à-vis the gray ones; Auger analyses have shown a thinner alumina film on the blue material (see above), thereby indicating a greater starting residual aluminum content in the alloy at the time of exposure. The higher aluminum content will increase the time to sulfidation (breakaway). In the same way, the amount of residual aluminum in the filter material preoxidized at 1000°C could be less than what is found in the specimens preoxidized at 800°C and may explain the greater corrosion susceptibility of the former.

The comparison of results from the specimens placed on the dirty- and clean-gas sides, respectively, of the filtration system at the Wabash River gasification plant provides important supporting information regarding the corrosion failure mechanism. As expected, deposits were heavier for those specimens exposed on the dirty-gas side (Table I). However, the extent of corrosion (formation of Fe-S, see above) did not depend on specimen placement. This observation is consistent with the sulfidation degradation mode described above and indicates that the corrosion mechanism is associated with gaseous sulfur and oxygen species rather than the char per se.

As described in the Results section, the preoxidized FAL (Fe-28% Al-5% Cr-0.1%Zr) o-rings were not substantially degraded after exposure for up to 6212 h on the clean-gas side and up to 4335 h on the dirty-gas side of the filtration system – only a relatively small amount of Fe-S was observed. In contrast, after approximately 2000 h, Fe-S was already starting to form in preoxidized filter o-rings made from FAS-Zr powder. Higher chromium concentrations in Fe_3Al-based alloys degrade sulfidation resistance at higher temperatures (DeVan 1989, DeVan and Tortorelli 1993), but may play a beneficial role in this lower temperature gasification plant environment by promoting alumina formation in cases where the oxidized layer is disrupted and/or by improving corrosion resistance at ambient temperatures during downtime (Buchanan et al. 1996). Effects of downtime corrosion can significantly negatively affect subsequent elevated temperature sulfidation (Bakker and Stringer 1997, Saunders et al. 1997b) and may have played a role in the present case for those specimens that saw more than one run cycle during plant exposure. For these reasons, an alumina-forming FeCrAl type of alloy (~20% Cr-5-10% Al) may offer better overall corrosion resistance at the relatively low operating temperatures of the gasification filter system.

Summary and Conclusions

Because of their good to excellent high-temperature corrosion resistance in sulfur-bearing environments, iron aluminide alloys are being evaluated as a potential material of construction for metallic filters to be used to clean fossil-fuel-derived gases prior to their introduction into gas turbines. Iron-aluminide filter-element or o-ring specimens have been characterized after exposure at the Wabash River Plant for times of approximately 400 to 6200 h. Several variables appear to be important to the length of service of these filters, including the preoxidation conditions during fabrication of the filter, time and temperature of exposure, and composition of the iron aluminide. The general mode of corrosion failure involves the formation of iron sulfide that grows into and occludes the pores, resulting in blockage of the filter and reduction in mechanical strength. This process appears to be accelerated at longer exposure times, possibly due to the depletion of aluminum from the filter alloy matrix and the resulting breakdown of the protective alumina layer and its inability to reform. However, with appropriate preoxidation treatments (those that produce a thin protective surface alumina), iron-aluminide filters can have extended lifetimes in coal-derived synthesis-gas environments.

A comparison of o–rings exposed on the clean- and dirty-gas side of the unit showed similar corrosion rates and indicated that the heavier surface deposits produced during exposure on the dirty-gas side does not affect the corrosion process to a significant degree. The filter material of iron aluminide with a higher chromium content tended to experience less degradation. One of these showed good resistance to 6212 h. The limited hoop-strength data generated to date have shown that iron-aluminide filters maintain their original strength as long as Fe-S formation has not occluded more than approximately 50% of the pores.

Acknowledgements

This work at Oak Ridge National Laboratory was sponsored by the Office of Fossil Energy, Advanced Research Materials Program, U.S. Department of Energy under Contract DE-AC05-

00OR22725 with UT-Battelle, LLC. The authors thank J. A. Horton and B. A. Pint for comments on the manuscript and D. N. Braski, H. L. Meyer, and L. R. Walker for their Auger and microprobe analyses.

References

Alvin, M. A., 1997. Performance and Stability of Porous Ceramic Candle Filters During PFBC Operation. *Mater. at High Temp.* 14: 285-94.

Bakker, W. T., 1998. Corrosion of Iron Aluminides in HCl Containing Coal Gasification Environments. *Corrosion/98,* NACE Intern., Houston, TX: paper number 185.

Bakker, W. T., and Stringer, J., 1997. Mixed Oxidant High Temperature Corrosion in Gasifiers and Power Plants. *Mater. High Temp.* 14: 35-42.

Blough, J. L., and Seitz, W. W., 1997. Fireside Corrosion Testing of Candidate Superheater Tube Alloys, Coatings, and Claddings — Phase II. *Proc. of Eleventh Annual Conference on Fossil Energy Materials*, Oak Ridge National Laboratory, Oak Ridge, TN: 357-366.

Buchanan, R. A., Kim, J. G., Ricker, R. E., and Heldt, L. A., 1996. Ambient Temperature Corrosion and Corrosive Sensitive Embrittlement. *Oxidation and Corrosion of Intermetallic Alloys*, Purdue University, West Lafayette, IN: 351-419.

DeVan, J. H. 1989. Oxidation Behavior of Fe_3Al and Derivative Alloys. *Oxidation of High-Temperature Intermetallics*, The Mineral, Materials, and Metals Society, Warrendale, PA: 107-115.

DeVan, J. H., and Tortorelli, P. F., 1993. Oxidation/Sulfidation of Iron-Aluminum Alloys. *Mater. High Temp.* 11: 30-35.

Gesmundo, F., et al., 1994. Corrosion of Fe-Al Intermetallics in Coal Gasification Atmospheres. *Materials for Advanced Power Engineering*, Kluwer Academic Publishers: 1657-67.

Lara-Curzio, E., 1999. Oak Ridge National Laboratory, Oak Ridge, TN, unpublished results.

McKamey, C. G., DeVan, J. H., Tortorelli, P. F., and Sikka, V. K., 1991. A Review of Recent Developments in Iron-Aluminum Alloys. *J. Mater. Res.* 6: 1779-1805.

Natesan, K., and Tortorelli, P. F., 1997. High-Temperature Corrosion and Applications of Nickel and Iron Aluminides in Coal-Conversion Power Systems. *International Symposium on Nickel and Iron Aluminides: Processing, Properties, and Applications*, ASM Intern., Materials Park: 265-280.

Nieminen, M., Kangasmaa, K., Kurkela, E., and Ståhlberg, P., 1996. Durability of Metal Filters in Low Sulphur Gasification Gas Conditions. *High Temperature Gas Cleaning*, Universität Karlsruhe, Karlsruhe, Germany: 120-31.

Oakey, J. E., et al., 1997. Grimethorpe Filter Element Performances -- The Final Analysis. *Mater. High Temp.* 14: 301-11.

Pint, B. A., 2000. Oak Ridge National Laboratory, Oak Ridge, TN, unpublished results.

Quadakkers, W. J., and Bongartz, K., 1994. Oxidation Lifetimes. *Werkst. Korros*. 45: 232-38.

Quick, N. R., and Weber, L. D., 1995. Accelerated-Life Testing of Sintered Filters for High-Temperature Corrosive Environments. *Proc. Second International Conf. on Heat Resistant Materials*, ASM Intern., Materials Park, OH: 663-71.

Saunders, S.R.J., *et al.*, 1997a. Behavior of Fecralloy and Iron Aluminide Alloys in Coal Gasification Atmospheres Containing HCl. *Mater. Sci. Forum* 251-254: 583-89.

Saunders, S.R.J., Gohil, D. D., and Osgerby, S., 1997b. The Combined Effects of Downtime Corrosion and Sulphidation on the Degradation of Commercial Alloys. *Mater. High Temp.* 14: 167-73.

Tortorelli, P. F., and DeVan, J. H., 1996. Oxidation and Other Corrosion Phenomena at Intermediate Temperature. *Oxidation and Corrosion of Intermetallic Alloys*, Purdue University, West Lafayette, IN: 267-331.

Tortorelli, P. F., Lara-Curzio, E., McKamey, C. G., Pint, B. A., Wright, I. G., and Judkins, R. R., 1998. Evaluation of Iron Aluminides for Hot Gas Filter Applications. *Proc. Advanced Coal-Based Power and Environmental Systems*, U. S. Department of Energy: paper PB7.

Tortorelli, P. F., McKamey, C. G., Lara-Curzio, E., and Judkins, R. R., 1999. Iron-Aluminide Filters for Hot-Gas Cleanup. *Proc. International Gas Turbine and Aeroengine Congress & Exhibition*, ASME Intern., New York: paper 99-GT-268.

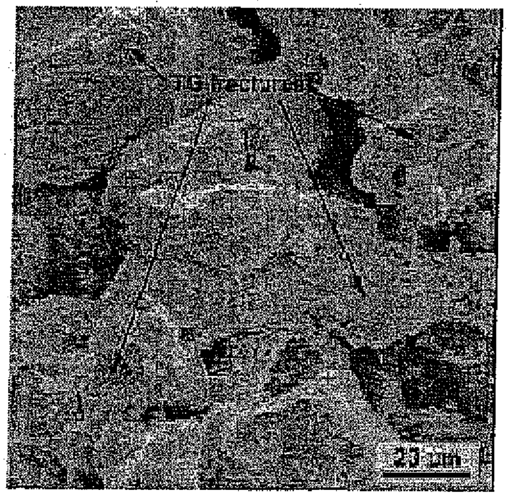

Fig. 1. SEM micrograph of as-fabricated FAS-Zr filter material (IA-187) showing transgranular failure through fully sintered material and oxide particles on powder surfaces.

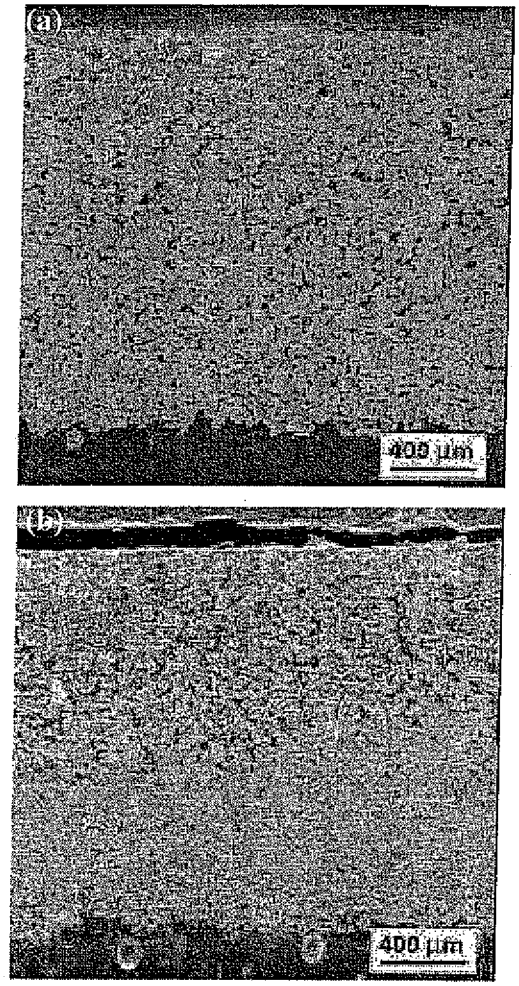

Fig. 2. Microstructures of two different samples of filter DC-20 exposed 1565 h in the Wabash River Energy Ltd plant; (a) showing normal porosity and (b) showing low inner surface porosity. Outer surface (gas inlet side) of filter is at top, inner surface (gas outlet) at bottom.

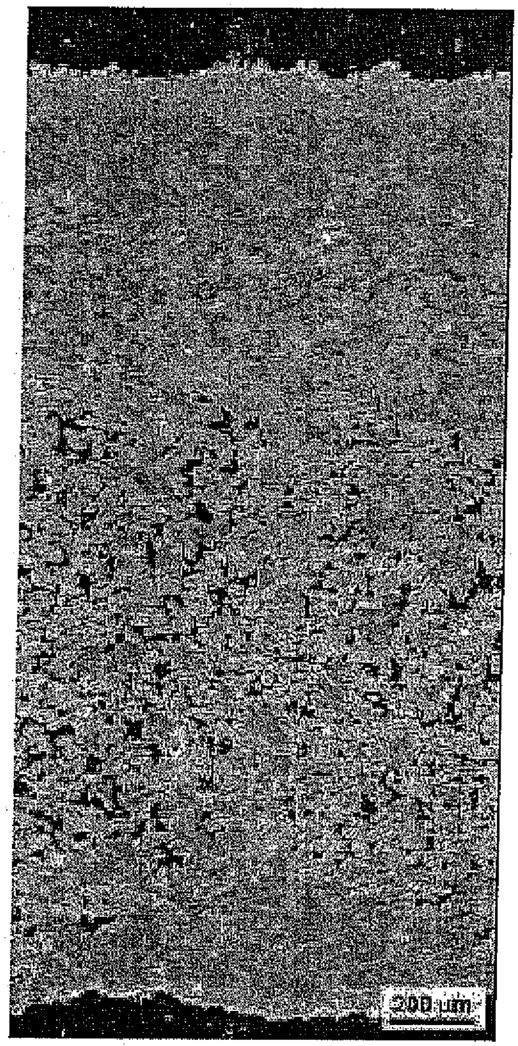

Fig. 3. Microstructure of filter DC-88 exposed for 2185 h in the Wabash River plant.

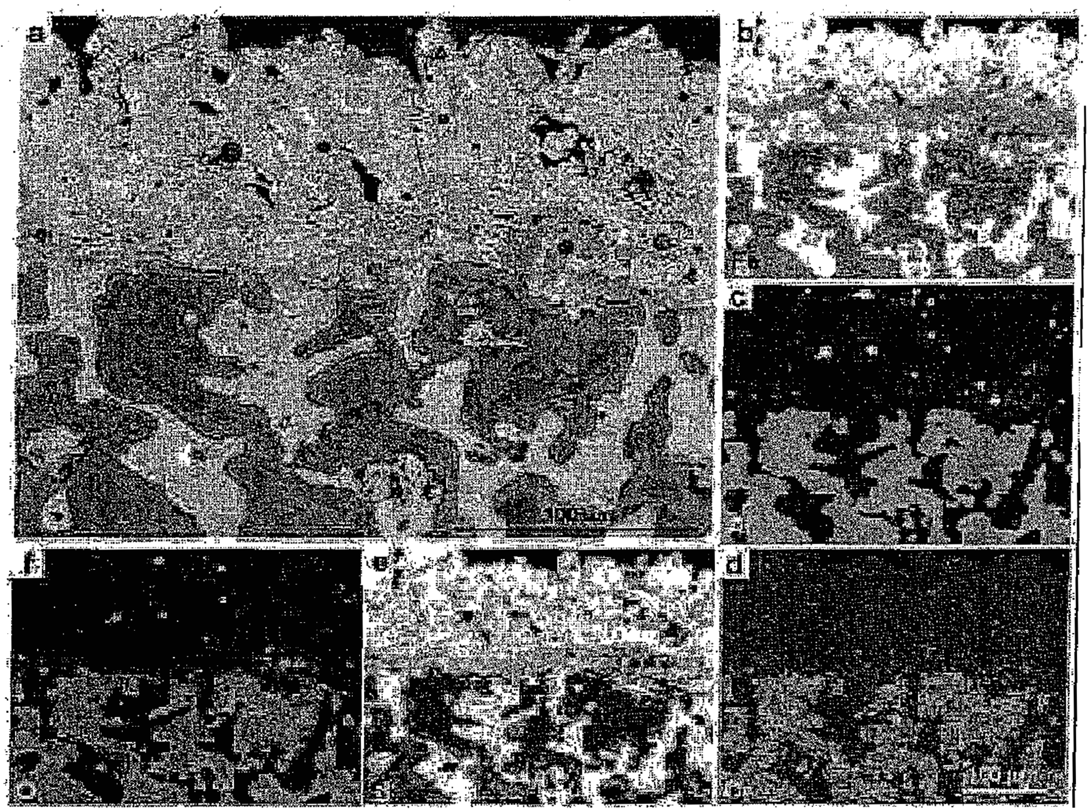

Fig. 4. Backscattered electron image (a) and x-ray mapping for (b) Fe, (c) Al, (d) Cr, (e) S, and (f) O in the outer region of filter DC-88.

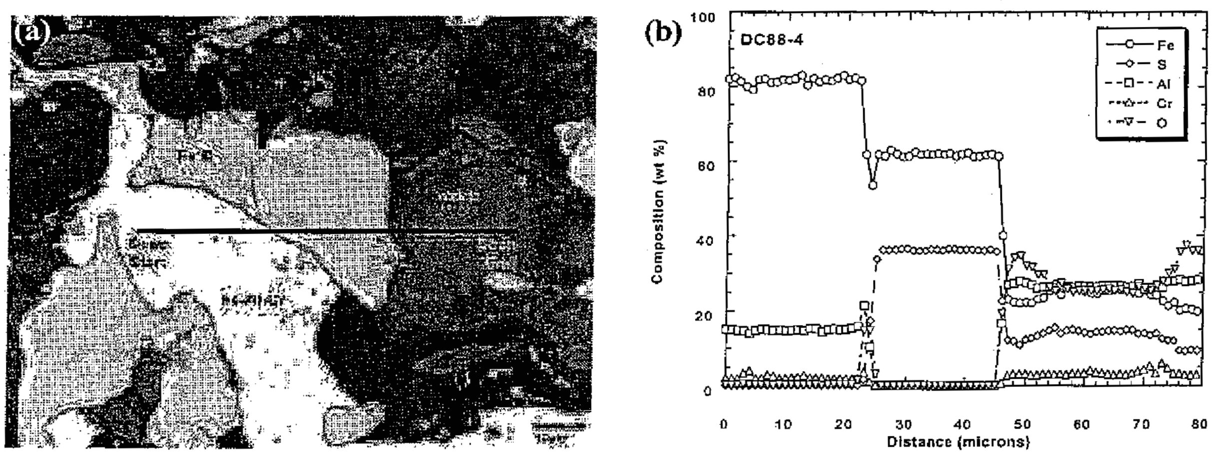

Fig. 5. Backscattered electron micrograph (a) and x-ray scan for Fe, S, Al, Cr, and O (b) across the three different phases observed in filter DC-88 exposed for 2185 h in the Wabash River plant.

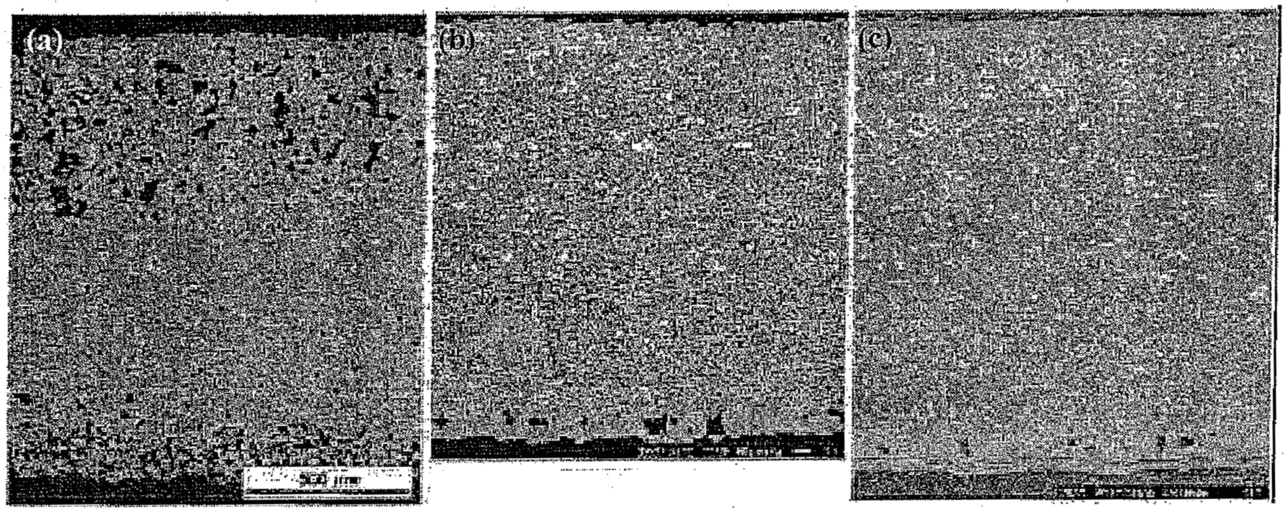

Fig. 6. Optical micrographs showing the microstructures of as-fabricated Fe-Al filters (a) IA-188 after 1628 h, (b) IA-187 after 2237 h, and (c) IA-187 after 3865 h of exposure on the clean-gas side of the Wabash River Plant. Magnifications of (b) and (c) are the same as (a).

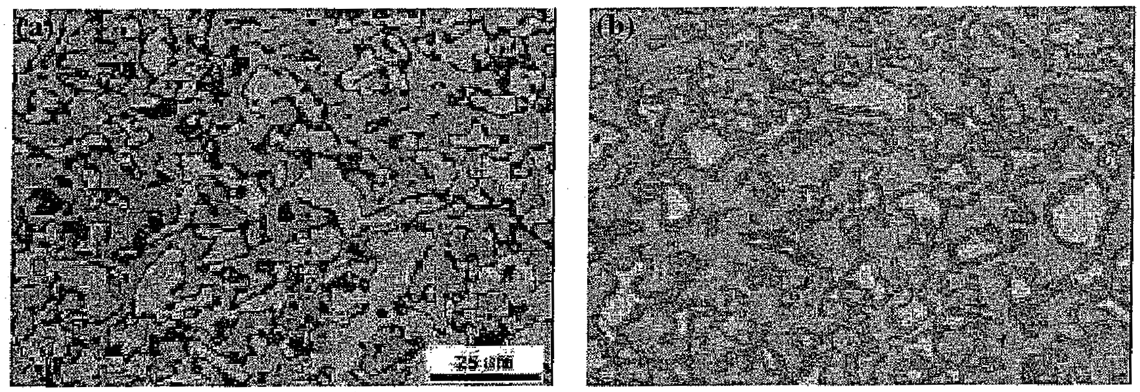

Fig. 7. High magnification optical micrographs showing the microstructures of as-fabricated Fe-Al filters (a) IA-188 after 1628 h and (b) IA-187 after 3865 h of exposure on the clean-gas side of the Wabash River Plant. Magnification of (b) is the same as (a).

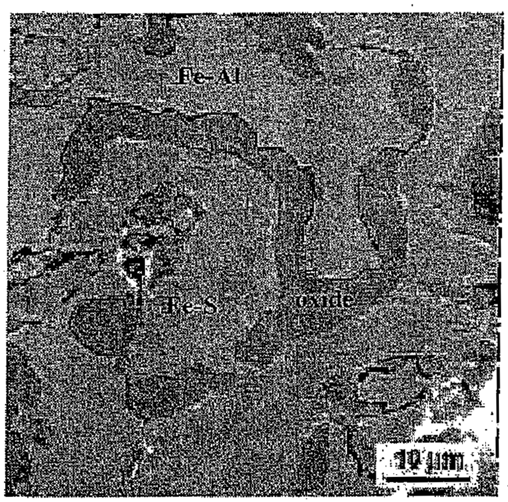

Fig. 8. High magnification optical micrograph showing formation of Fe-S and Al-O phases in as-fabricated Fe-Al filter IA-188 exposed for 1628 h in the Wabash River Plant. White particles in the Fe-S phase are arsenic.

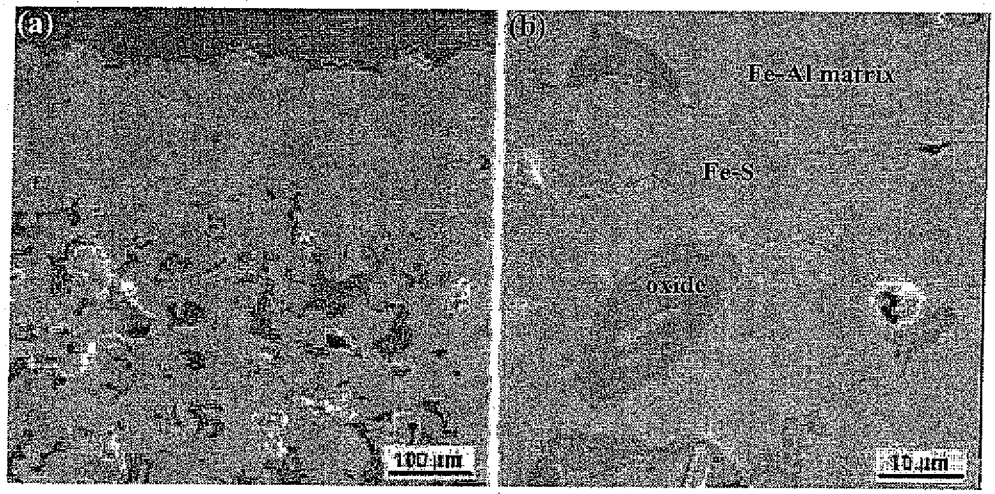

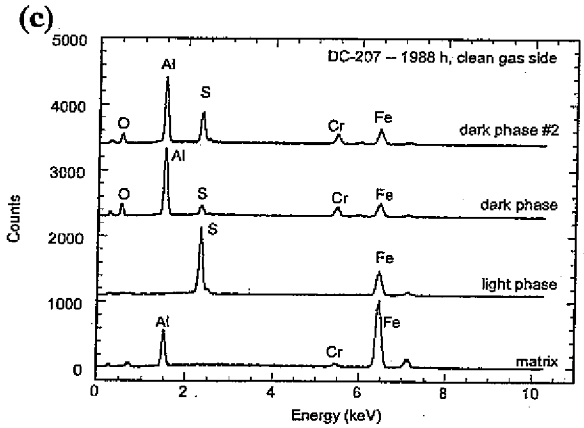

Fig. 9. Low- (a) and high-magnification (b) SEM micrographs and (c) EDS spectra for phases present in DC-207 exposed for 1988 h on the clean-gas side.

Fig. 10. Iron-sulfur particles forming inside pores in the interior of o-ring DC-207 exposed for 1988 h on the clean-gas side.

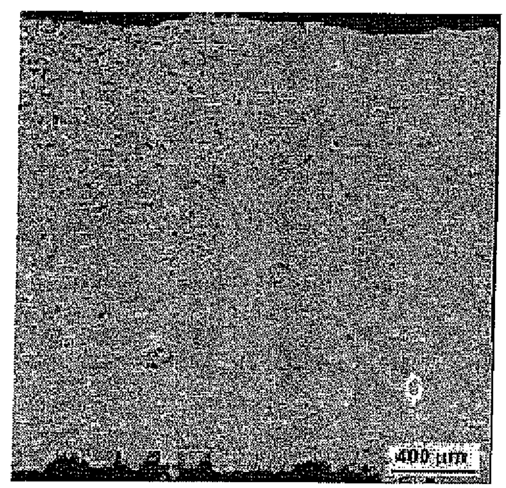

Fig. 11. SEM micrograph showing blocked pores in o-ring DC-209 (from gray filter) after exposure for 1988 h on the clean-gas side of the Wabash River Plant.

Table I. Fe-Al Filter Material Exposed at the Wabash River Plant

Filter Design	Pre-oxidation Temp. (°C)	Exposure time (h)	Exposure details[d]	Results of microstructural analyses	Fracture strength (kN)
IA-187 IA-188 IA-191 IA-141	As fabricated As fabricated 800 1000	None None None None		40-50% porous; oxide particles on pore surfaces; oxide coating on surfaces of 0.5-3 microns thickness; ligaments averaged 6-10 microns	2.0
DC-20[a]	800	574	Vessel	Light surface deposits, some regions of non-uniform porosity	2.0
DC-36[a]	800	1565	Vessel	Non-uniform porosity, pores may be blocked	1.6
DC-88[a]	800	2185	Vessel, 250h petcoke	Fe-S outer layers, blocking gas flow	1.4
IA-188[b]	As fabricated	1628	Clean	Filter blocked by Fe-S throughout inner 2/3 of filter	1.1
IA-187[b]	As fabricated	2237	Clean, 100h petcoke	Filter blocked throughout, thicker deposit on inner surface	
IA-187[b]	As fabricated	3865	Clean, 100h petcoke	Completely full of Fe-S, thick layers on both sides, filter blocked	
DC-207[b]	800	1988	Clean, all petcoke	No surface deposits, large Fe-S layers blocking gas flow, medium interior corrosion	2.2
IA-191[b]	800	2237	Clean, 100h petcoke	No deposits, some Fe-S, filter OK	2.2
DC-205[b]	800	4335	Clean, last ~3000-3500h petcoke	OK, no deposits, some Fe-S throughout	2.2
IA-141[b]	1000	2237	Clean, 100h petcoke	Lots of Fe-S throughout, scattered open pores, may still be filtering	
IA-141[b]	1000	3865	Clean, 100h petcoke	Completely full of Fe-S, thick layers on both sides	
DC-208[b]	800 (blue)	1988	Clean, all petcoke	Light deposit, light corrosion, pores open	2.3
DC-211[b]	800 (blue)	1988	Dirty, all petcoke	Heavy deposit, light corrosion, pores open	2.2
DC-209[b]	800 (gray)	1988	Clean, all petcoke	Medium deposit, heavy corrosion, pores blocked	0.9
DC-210[b]	800 (gray)	1988	Dirty, all petcoke	Heavy deposit, significant corrosion, filter may be blocked	1.5
DC-192[b]	800 (FAL)[c]	2347	Clean, 1000-1500h petcoke	Light-to-medium surface deposits, light corrosion, pores open	1.5
DC-193[b]	800 (FAL)[c]	6212	Clean, 1000-1500h petcoke	Light-to-medium surface deposits, light corrosion, pores open	2.2
DC-195[b]	800 (FAL)[c]	2347	Dirty, 1000-1500h petcoke	Medium-to-heavy surface deposits, light corrosion, pores open	1.4
DC-206[b]	800 (FAL)[c]	4335	Dirty, last ~3000-3500h petcoke	Heavy deposits, light corrosion, pores open	2.0

[a]Specimen from filter element.
[b]Specimen was o-ring cut from filter element.
[c]FAL composition = Fe-28at.%Al-5at.%Cr.
[d]Clean = clean-gas side; dirty = dirty-gas side.